UNIVERSITY OF PARDUBICE

FACULTY OF CHEMICAL TECHNOLOGY

Institute of Environmental and Chemical Engineering

Olga Krupková

Application of advanced oxidation processes and membrane processes in wastewater and process water treatment

Theses of the Doctoral Dissertation

Pardubice 2024

Study program: **Chemical and Process Engineering**

Study field: **Environmental Engineering**

Author: **Olga Krupková**

Supervisor: **doc. Ing. Libor Dušek, Ph.D.**

Year of the defence: **2024**

References

KRUPKOVÁ, Olga. Application of advanced oxidation processes and membrane processes in wastewater and process water treatment. Pardubice, 2024. Dissertation thesis (Ph.D.). University of Pardubice, Faculty of Chemical Technology, Institute of Environmental and Chemical Engineering, Supervisor doc. Ing. Libor Dušek, Ph.D.

Abstract

The theoretical part is focused on wastewater from the textile industry and on the issue of its treatment. This is followed by a description of the separation technology, specifically membrane processes and the formation of hydroxyl radicals using advanced oxidation processes. Furthermore, the model organic dyes used, which are difficult to biodegrade, are described. The thesis also contains a detailed description of reaction kinetics, which was subsequently used for calculations. The theoretical part is followed by the experimental part, which contains a description of the device, methodology and results of the whole work. The conclusion summarizes the efficiency of the processes used to degrade synthetic dyes and their advantages for application in industry.

Abstrakt

Teoretická část je zaměřena na odpadní vody z textilního průmyslu a na problematiku jejich čištění. Poté následuje popis separační technologie, konkrétně membránových procesů a tvorba hydroxylových radikálů pomocí pokročilých oxidačních procesů. Dále jsou zde popsány použitá modelová organická barviva, která jsou obtížně biologicky odbouratelná. Práce obsahuje i podrobný popis reakční kinetiky, který byl následně i využit pro výpočty. Na teoretickou část navazuje experimentální část, která obsahuje popis zařízení, metodiku a výsledky celé práce. V závěru je shrnuta efektivita použitých procesů na odbourání syntetických barviv a jejich výhody pro aplikaci v průmyslu**.**

Keywords

Textile wastewater, textile dyes, advanced oxidation processes, membrane processes, Fenton reaction

Klíčová slova

Textilní odpadní vody, textilní barviva, pokročilé oxidační procesy, membránové procesy, Fentonova reakce

Table of Contents

Introduction

Advanced Oxidation Processes (AOPs) are processes that use hydroxyl radicals that have a strong oxidizing effect to remove otherwise hard-to-decompose substances. AOPs have found a wide range of applications in the treatment of industrial wastewater, groundwater, and leachate from landfills. Membrane processes are an economically equivalent substitute for separation processes, where the main advantages are their high separation efficiency at ambient temperature, without the use of additional chemicals. In addition, membrane processes show lower energy consumption and space-saving requirements [1, 2].

This thesis is devoted to the application of the already mentioned processes in the treatment of wastewater and process water, specifically water from the textile industry. Solutions of model dyes were subjected to their degradation using advanced oxidation processes and separation using membrane processes.

1. Theoretical part

1.1. Wastewater from the textile industry

The textile industry is one of the largest and most complex industrial chains in the manufacturing industry. Textile production requires several stages of mechanical processing, such as spinning, knitting, weaving, and garment production, which are isolated from wet processing processes such as sizing, desizing, washing, bleaching, mercerizing, dyeing, printing, and finishing, but there is a link between dry processes and successive wet processing processes. A wide range of pollutants leave the textile industry from all stages of production including wastewater, solid waste, and air emissions. The main environmental problems in the textile industry are the amount of water discharged and the chemical burden that this industry entails. Overall, the textile industry is very water intensive. Water is used for the cleaning of raw materials and for many flushing steps throughout the production process [3, 4, 5].

1.2. Description of the selected membrane process

Membrane processes are used for concentration or purification of dilute solutions and dispersions, where a specific feature of these processes is the use of a semipermeable membrane as a separation element, which exhibits high selectivity, high permeability and long service life. The selectivity of the membrane affects the separation efficiency and purity of the obtained components. Low selectivity requires a multi-stage operation and thus increases the economic demands of the process. The permeability of the membrane affects the speed of the process and the size of the membrane area. Low permeability can be compensated for by a larger membrane area, but this will also increase investment costs. The lifetime of the membrane is influenced by its mechanical, thermal and chemical resistance and the associated operating costs such as maintenance. In the membrane process, the raw material, hereinafter referred to as spraying, is fed in such a way that it is in contact with the active layer of the membrane. The component that passes through the membrane is called permeate and the retained component is

called retentate. Figure 1. The penetration rate of a given component or the selectivity of the process is determined by the different size of the separated particles, the size of the pores in the membrane, the diffusion or dissolution of the components in the active layer material, different surface properties such as charge, wettability, etc. [2, 6, 7, 8].

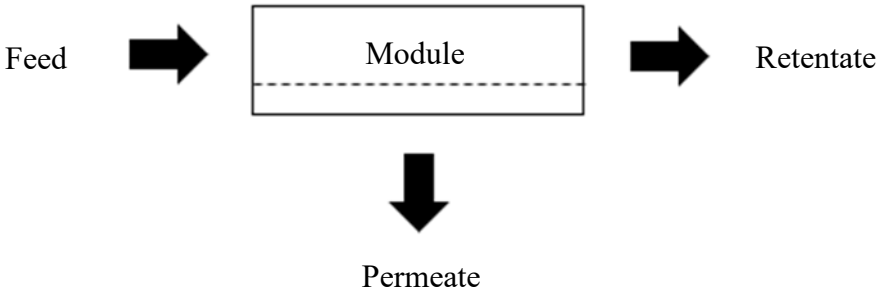

Figure 1 Scheme of the membrane process

1.2.1. Nanofiltration

Nanofiltration separates low-molecular-weight organic substances and multivalent ions from monovalent ones. Applied pressures range from 10-40 · 105 Pa. Unlike reverse osmosis, nanofiltration can be operated at lower pressures with higher permeate flux intensity. The thickness of the active layer is below 1 μm, and it is required to be as small as possible. The charge of the membranes and the pH of the environment affect the separation capabilities of nanofiltration membranes [9].

The selective layer of NF membranes is porous, but the pores are small (<2 nm). Materials suitable for nanofiltration membranes are hydrophilic polymers, the most used are composite membranes with a polyamide selective layer, the cross-section of which is shown in Figure 2, or with a cation-selective layer (usually sulfonated polysulfone). The selective layer carries a strong negative charge [2, 9, 10, 11].

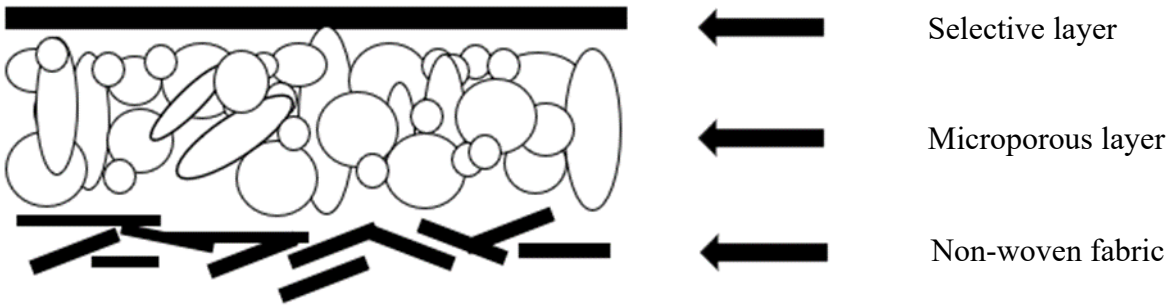

Figure 2 Illustration of nanofiltration composite membrane layers

1.3. Photochemical reactions

1.3.1. UV light and its classification

To induce photochemical changes in the molecule, we irradiate the reaction system during the oxidation process with electromagnetic radiation in the UV-VIS region. The visible spectrum covers wavelengths between 400 and 800 nm, lit. [12, 13].

The UV region is usually divided into four regions:

• UV-A (called near-UV radiation), whose wavelengths range from 315 to 400 nm.

• UV-B has a wavelength range from 280 to 315 nm.

• UV-C (short UV) includes wavelengths shorter than 280 nm.

• VUV (vacuum ultraviolet light) has wavelengths lower than 200 nm, sometimes classified under UV-C

A UV source that would ensure an efficient course of the oxidation reaction should have an emission spectrum of wavelengths below 260 nm. Suitable sources for processes based on the UV+ H_2O_2 system low-pressure mercury lamps and UV-vacuum lamps appear to be [14].

1.3.2. System of UV + H_2O_2

Photoinduced decomposition of hydrogen peroxide in pure water takes place by a radical mechanism, where hydroxyl radicals formed by homolytic cleavage of the O-O bond initiate a series of reactions characterized by an initiation step, see Equation (1). This is followed by the propagation step, which is described by equations (2) to (3). Finally, termination reactions involve radical recombination, see equations (4-6). The efficiency of ·OH radical production depends on the ability of hydrogen peroxide to absorb UV radiation, as well as on the physical and chemical properties of the liquid that undergoes the oxidation process [14, 15, 16].

$$H_2O_2 + h\nu \rightarrow 2HO\cdot \quad (1)$$

$$H_2O_2 + HO\cdot \rightarrow H_2O + HO_2 \quad (2)$$

$$HO\cdot_2 + H_2O_2 \rightarrow H_2O + O_2 + HO\cdot \quad (3)$$

$$HO\cdot + HO\cdot \rightarrow H_2O_2 \quad (4)$$

$$HO\cdot + HO\cdot_2 \rightarrow H_2O + O_2 \quad (5)$$

$$HO\cdot_2 + HO_2 \rightarrow H_2O_2 + O_2 \quad (6)$$

1.3.3. Photo-Fenton reaction

The reagents used for the photo-Fenton reaction are ferrous or ferric ion (mainly sulphate or ferrous chloride ($Fe^{2+)}$ and less commonly ferric sulphate or nitrate (Fe^{3+})) and hydrogen peroxide. The efficiency of the process depends on the pH, temperature, and concentration of both reagents used**.** In general, a higher concentration of hydrogen peroxide and iron ions causes a higher rate of oxidation, but an excess of iron ions or H_2O_2 limits or inhibits the efficiency of the process. In this case, reactions take place that reduce the concentration of hydroxyl radicals, see equations (7) and (8), lit. [17, 18].

$$Fe^{2+} + HO\cdot \rightarrow Fe^{3+} + HO\cdot \quad (7)$$

$$H_2O_2 + HO\cdot \rightarrow H_2O + HO^{\cdot}{}_2 \quad (8)$$

The normal concentration of iron ions used for the photo-Fenton reaction in water decontamination is in the range from 0.01 to 1 mmol/L, which increases the reaction rate as the concentration of iron ions increases. Due to the effect of pH on the solubility of Fe^{2+} and Fe^{3+}, most iron ions precipitate at a slightly acidic pH and higher. At the same time, dispersed insoluble aggregates and colored suspended solids are formed to prevent the passage of light, which also reduces the efficiency of microbial oxidation [17]. A scheme of the application of the photo-Fenton reaction for wastewater disinfection is shown in Figure 3.

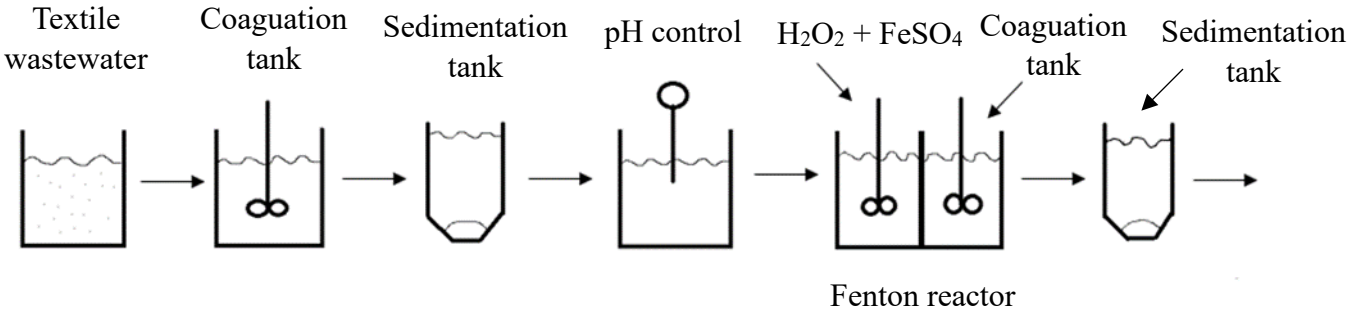

Figure 3 Diagram of the implementation of the photo-Fenton reaction for wastewater disinfection

2. Experimental part

2.1. Selected model dyes

2.1.1. Acid Blue 80

Acid Blue 80 is an anthraquinone dye that is water-soluble and has been used as a model pollutant organic for this work. Industrially, AB 80 is used for dyeing wool and nylon. The structural formula of the dye shown in Figure 4 indicates that the dye is present in the form of a disodium salt**.** This also corresponds to the molecular formula of the dye $C_{32}H_{28}N_2Na_2O_8S_2$ and its molecular weight of 678.68 g/mol. AB80 is a highly resistant dye to biological degradation. In aqueous media, it exhibits an absorption maximum at a wavelength λ_{max} of 627 nm [19, 20, 21].

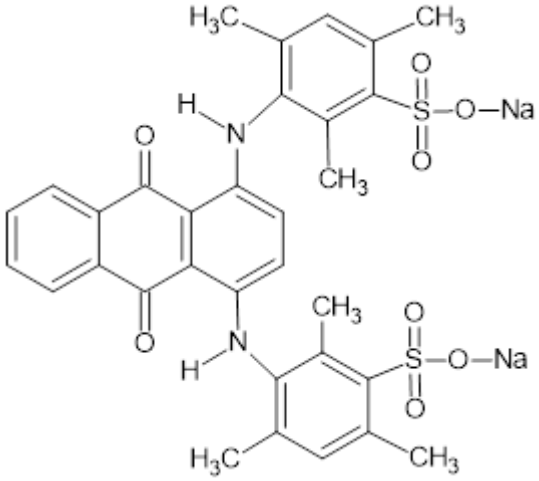

Figure 4 Structure of Acid Blue 80

2.1.2. Acid Green 25

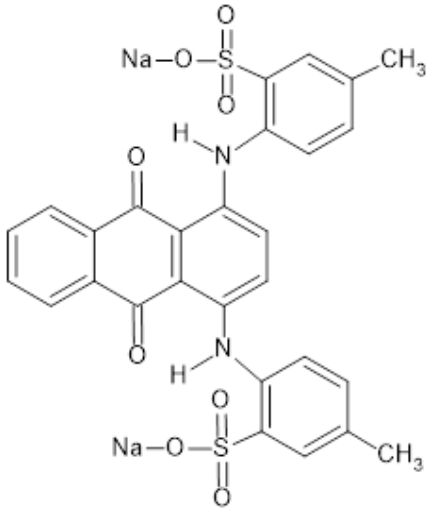

Figure 5 Structure of Acid Green 25

Acid Green 25 is an aminoanthraquinone dye with a molecular weight of 622.58 g/mol. The high stability of this dye is due to the formation of a hydrogen bond between the amino group at position 1 and the carbonyl group. Acid Green 25 is a cationic dye that is used to dye polyacrylonitrile fibers. The dye formula is shown in Figure 5 above [22, 23].

2.1.3. Reactive Blue 49

Reactive dye Reactive Blue 49 is used in the textile industry for dyeing wool, cotton, viscose, polyamide and silk. RB49 has a high molecular weight of 882.182 g/mol and its structure is shown in Figure 6 [24, 25, 26].

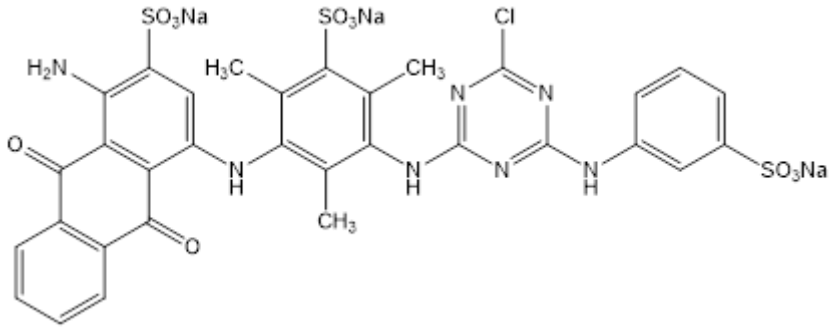

Figure 6 Structure of Reactive Blue 49

2.1.4. Acid Red 118

Azo dye Acid Red 118 belongs to the class of acid dyes. It is used for dyeing wool, polyamide, and silk. The molecular weight of AR118 is 562.59 g/mol. The structural formula of the dye is shown in Figure 7 [27, 28].

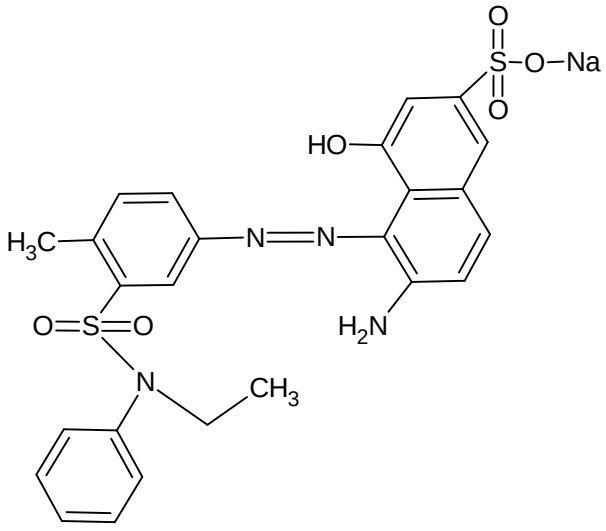

Figure 7 Structure of Acid Red 118

2.1. Experimental equipment

2.1.1. Device for nanofiltration

A Crossflow unit FT18-RO/UF Armfield (Great Britain) containing an NF membrane module (FT 18, Armfield, GB) was used for nanofiltration separation of model waste substances, see Fig. 8. The device consisted of a stainless-steel storage tank with a volume of approx. 12 L, from which the injection was led via two piston pumps to the Micro 240 membrane module from the manufacturer PCI membranes (Great Britain). The membrane module contained 2 tubular membranes in series connection. After passing through the module, the retentate passed through a back pressure regulator to regulate the set applied pressure difference during the experiment. After passing through the plate heat exchanger, the retentate returned to the storage tank. Furthermore, a cooling device was used to regulate the cooling water temperature (Tae Evo device from MTA S.p.A., Italy). The inlet temperature was maintained in the range of 25±0.5 °C. The permeate was drained from the membrane module into a collection beaker, which was set up on a balance connected to a computer. The apparatus was also equipped with a manometer, and the inlet temperature was regulated to a value determined using a bench-top conductometer (inoLab cond 7110, WTW, Germany) with a conductometric cuvette located in the injection tank. Permeate conductivity was measured using a portable conductometer (pH/cond 340i, WTW, Germany). Both conductometers were equipped with the same type of Tetracon 325 conductometric cell (WTW, Germany).

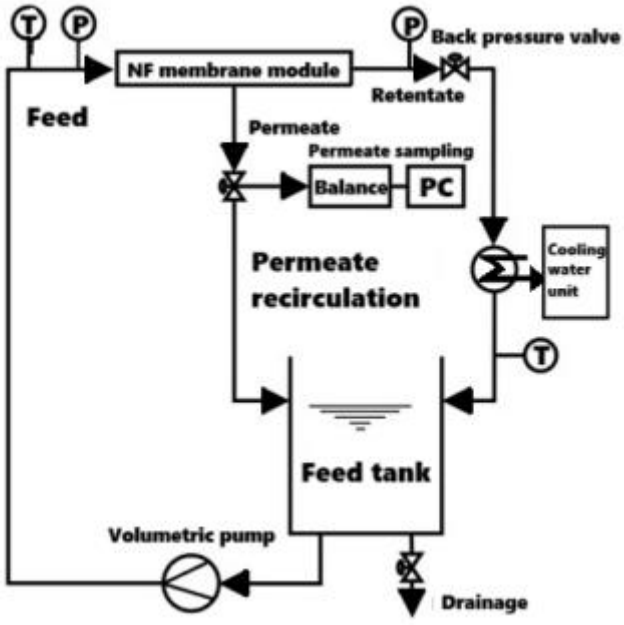

Figure 8 Diagram of the used nanofiltration apparatus

2.1.2. Photochemical equipment

The equipment for kinetic decolorization and mineralization experiments using the reaction system UV-C, UV-C/H_2O_2 or UV-C/H_2O_2/Fe^{2+} in homogeneous consisted of an electromagnetic stirrer, a storage tank with a volume of 5 l, tempered at 25±0.5 °C with a Julabo EH-5 thermostat and a UV-C radiation source, see Fig. 9. It was a low-pressure mercury discharge lamp EB-G45105 (supplier: AQUA, Czech Republic) with an energy consumption of 48 W (the total light output of the source was 13 W, area density luminous flux for 185 nm was 0.256 W/m^2, the area density of luminous flux for 254 nm was 1.20 W/m2). The UV-C source was connected to a storage tank in a closed circuit with a diaphragm pump with a bypass allowing to regulate the flow in the range of 0–1.3 L/min. All kinetic experiments were performed at a constant flow rate of the model solution V = 0.33 L/min through the UV-C source. The actual concentration of the model solutions was measured spectrophotometrically using a flow cell supplied by a peristaltic pump via a Libra S22 spectrophotometer with evaluation on a PC.

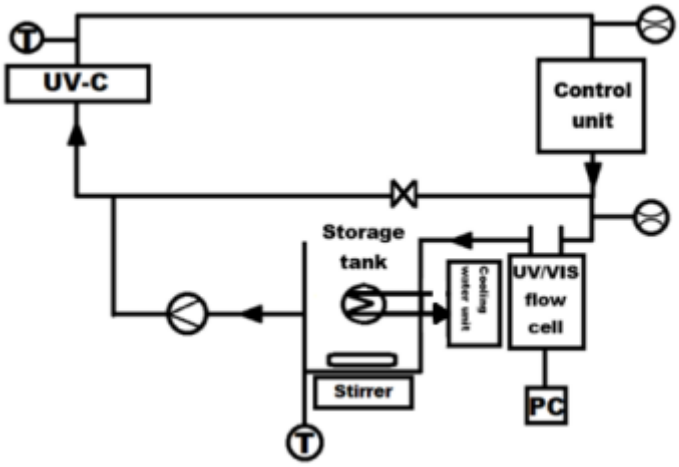

Figure 9 Diagram of the used photochemical apparatus

3. Results and Discussion

3.1. Nanofiltration

3.1.1. Effect of Reactive Blue 49 concentration

Figures 10 shows the obtained results in graphical form together with the dependence obtained in the demineralized water experiment. It can be noted that at the dye concentrations used, the intensity of the permeate flow is not significantly affected by its presence. Only at higher pressure differences and higher dye concentrations for the AFC 40 membrane does a slight decrease in the permeate flow occur. This decrease is due to the increase in the osmotic pressure of the dye and the osmotic pressure of the salt that is naturally present in the available commercial grade dye for the textile industry.

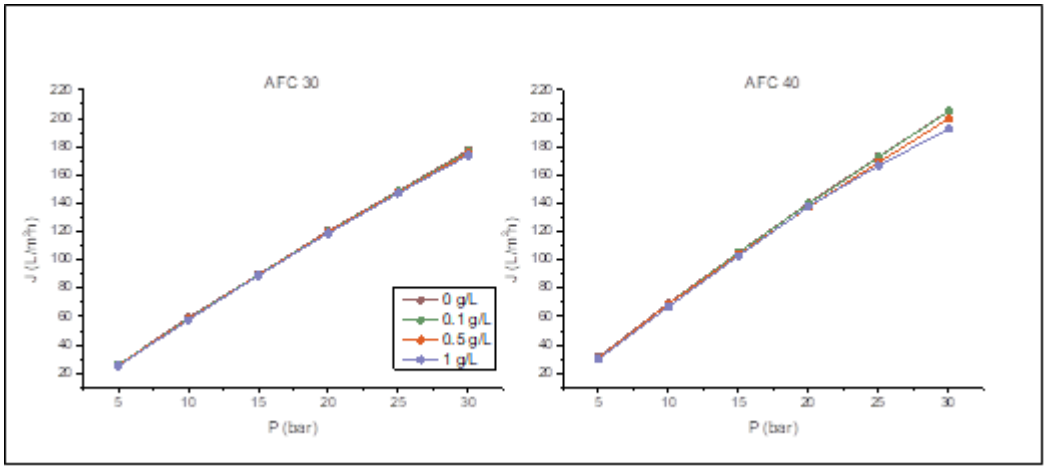

Figure 10 Permeate flow dependence on pressure difference for AFC 30 and AFC 40 membranes for individual concentrations of RB 49 dye.

3.1.2. Effect of Acid Blue 80 concentration

Figure 11 also shows the obtained results of the influence of the Acid Blue 80 dye concentration in a graphical form. Based on the previous results with the used membranes, only the AFC 40 membrane was used for further experiments with dyes. At lower concentrations, a smooth process of separation can be observed without any indication of increasing concentration on the membrane. However, at an AB80 concentration of 5 g/l at a pressure of 30 bar, there is an indication of the formation of a gel layer and pressure losses already occur. The limit permeate concentration was 4 mg/l for an initial concentration of 0.05 g/l dye in the spray, which corresponds to 91.81% rejection. Furthermore, the rejection was around 99.03% in the experiment with the initial concentration of the dye in the injection 0.5 g/l, the rejection with a value of 99.48% was measured in the experiment with the concentration of the dye in the injection 1 g/l and for the concentration of 5 g/l the AB80 dyes in the spray had a rejection of 99.9%.

Another series of measurements was with an initial concentration of 25 g/l AB80 in solution, but at different pH values of 5,6,7. Here, it was only measured up to a

maximum pressure of 20 bar, because the gel layer was already formed at a pressure above 10 bar. There are very slight differences in the values between 15 and 20 bars. In this series of experiments, the limit dye concentration of all measurements was around 20 mg/l, which corresponds to a rejection of 99.92%.

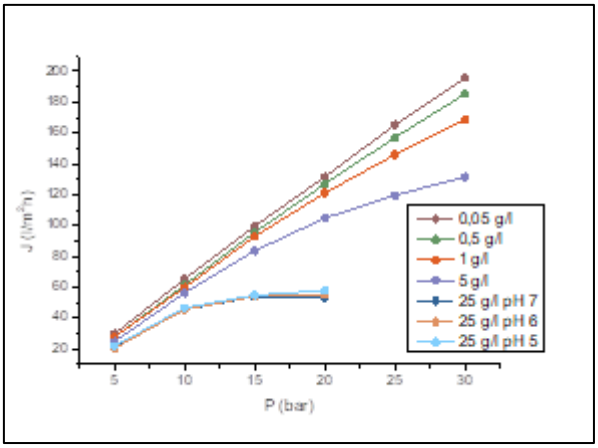

Figure 11 Dependence of the permeate flux on the pressure difference for AFC 40 for individual AB80 dye concentrations

3.1.3. Effect of Acid Green 25 concentration

On the figure 12 it can be noticed that at a lower applied concentration of the AG25 dye, there is apparently no increase in the concentration on the membrane in the permeate, and thus this separation was smooth. This is not the case for the initial dye concentration of 5 g/l in the spray, where no significant difference can be seen on the graph between the applied pressures of 25 and 30 bar, indicating an increase in concentration on the membrane. The limit concentration of the permeate in experiments with the dye AG 25 was 296 μg/l for an initial concentration in the permeate of 0.5 g/l, which corresponds to a rejection of 99.94%. For an initial AG25 concentration of 1 g/l in the injection, the rejection reached a value of 99.9%, and for an initial dye concentration of 5 g/l, the rejection was set at a value of 99.96%.

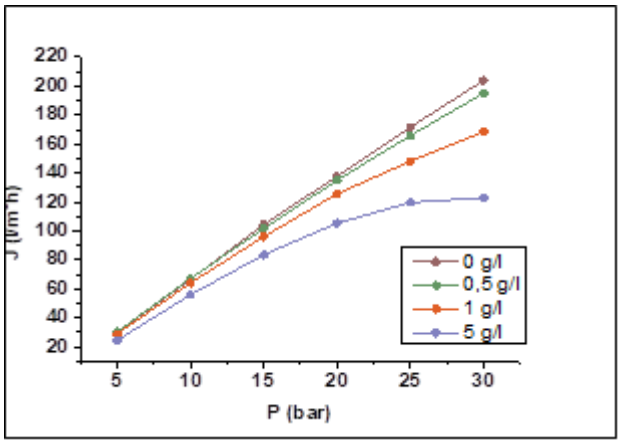

Figure 12 Dependence of the permeate flux on the pressure difference for AFC 40 for individual concentrations of AG25 dye

3.2. Photochemical degradation of dyes in the role of model waste substances

3.2.1. Reactive Blue 49

It can be stated that in the acidic region the decolorization process with the participation of UVC was relatively slow and the reaction half-time was approx. 2.3 h. After that, the decolorization rate increased in the pH range 5-9, which corresponded to reaction half-times of approx. 1.3 hours. In the alkaline region, decolorization by UV-C was relatively fast, as the value of the reaction half-time was t1/2 = 36 min, see also the pH profile for the UV-C reaction system in Figure 13.

By applying the UV-C/H_2O_2 reaction system, both the decolorization of the wastewater and the oxidation itself, and finally the mineralization of RB49, were accelerated to varying degrees, although again depending on the pH of the environment. In the case of discoloration, which was always quantitative in all cases, the half-time of the reaction varied from 26 min at pH = 11 to approx. 32-36 min for the pH range 3-9. The effect of environmental pH did not play a significant role here.

The photo-Fenton reaction is conditioned by the presence of dissolved Fe^{2+} ions in water, and therefore its use is limited to the acidic pH range. Nevertheless, the kinetic study was carried out in the range of pH 3-7, i.e. also in neutral pH, when the speed and quantity of precipitates formed due to their low concentration did not prevent the repetition of kinetic experiments. Due to the formation of ferric salts affecting the UV-VIS spectrum, it was necessary to compensate for this interference by a blind kinetic experiment without the presence of RB49. As for the decolorization of the dye, it was quantitative at pH=3 relative to the reaction system. It was also the fastest of all the kinetic experiments. The decolorization half-time of the model wastewater was 22.8 min. However, as the pH increases, the concentration of the available catalyst drops rapidly, and with it the rate of decolorization is roughly halved.

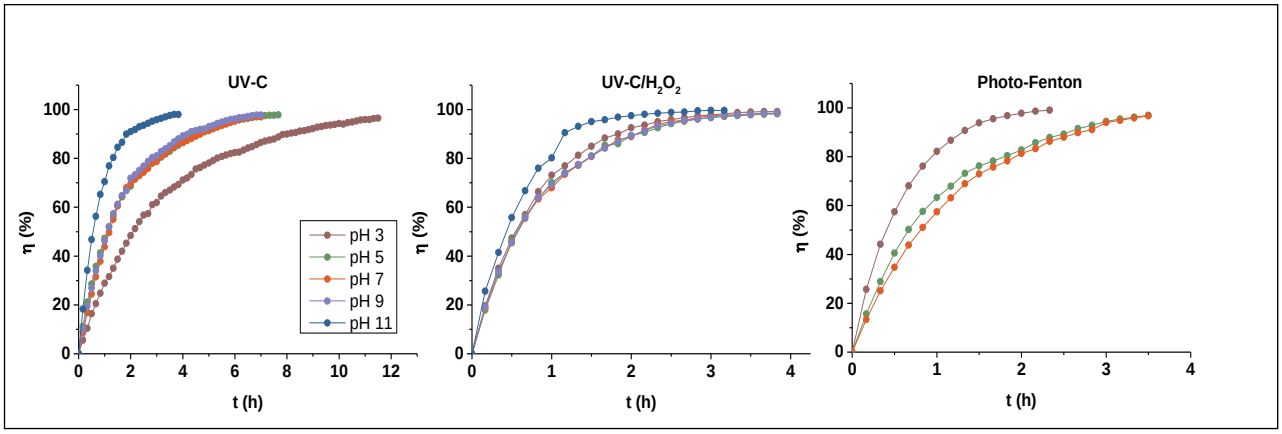

Figure 13 Dependences of the decolorization efficiency of RB49 aqueous solutions on time at different pH values and reaction systems at a temperature of 25 °C

During the kinetic experiments, the reaction mixture of the model wastewater containing RB49 was sampled, and the degradation intermediates were analyzed by LC-MS. As could be expected, next to the unreacted dye there was also the product of its hydrolysis, arising after the attack of the nucleophile on the carbon atom of the 6π electron triazene ring. The reaction proceeds by a nucleophilic bimolecular heteroaromatic substitution mechanism. By this mechanism, RB49 is also fixed to cellulosic material containing hydroxyl groups, which appear here in the nucleophile position. Here water played this role and the leaving nucleofuge (group) is Cl-. The reaction pathway proceeds according to the diagram in Fig. 14 [29].

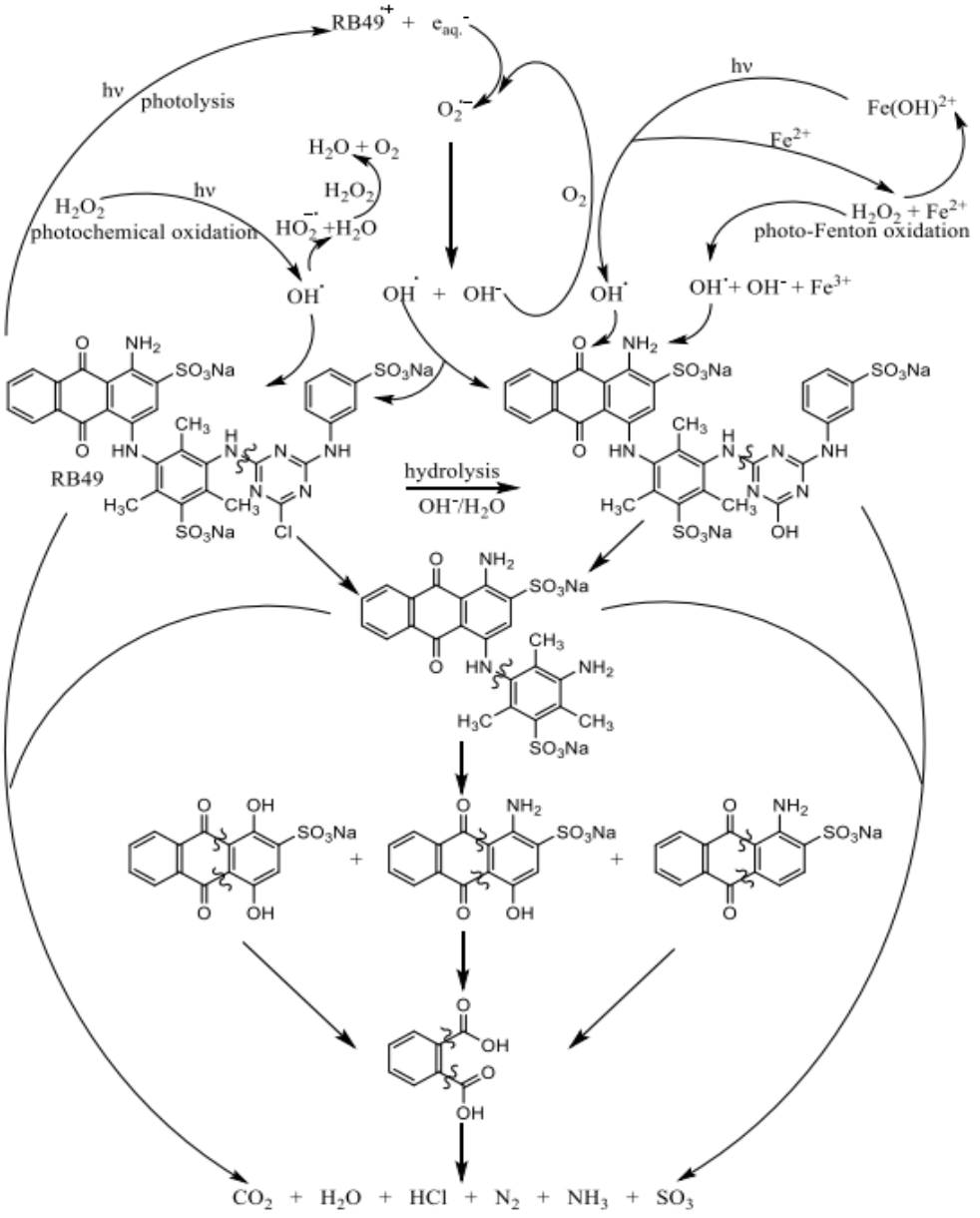

Figure 14 Decomposition of RB49 under hydrolysis and oxidation conditions in the presence of hydroxyl radical

3.2.2. Acid Blue 80

Time dependences of absorbance were obtained from the kinetic experiments, from which AB80 dye concentrations were calculated as a function of time using the calibration curve equation $A_{627} = 0.148c_{AB80} + 0.091$, $r^2 = 0.998$. Zero-, first-, and second-order kinetic equations were applied to interpret the kinetic data. In accordance with several analogous studies, the first-order rate constants proved to be the most suitable for describing the obtained dependencies. It can be stated that the decolorization of AB80 in the homogeneous phase took place quantitatively regardless of the selected reaction system in the entire tested pH range. This is also evident in Figure 47, which describes the decolorization efficiency of model wastewaters containing AB80 for reaction systems of photo-Fenton oxidation, simple photolysis, and photochemical oxidation in the presence of hydrogen peroxide as shown in figure 15**.**

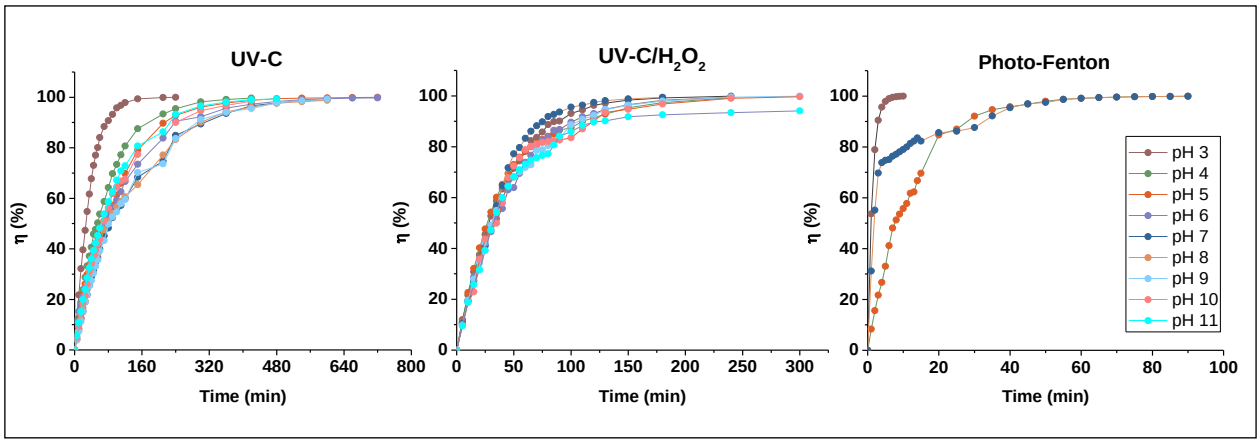

Figure 15 Dependences of decolorization efficiency of model wastewater containing Acid Blue 80 on time for reaction systems UV-C, UV-C/H_2O_2 and photo-Fenton reaction. Spectrophotometric kinetic measurements were performed at t= 25 ◦C, λanal= 627 nm and in the pH range between 3-11

3.2.3. Acid Green 25

From the AG25 dye solution kinetic decolorization experiments shown in fig. 16, AG25 dye concentrations as a function of time were calculated using the calibration curve equation $A_{643} = 0.1267c_{AG25}$, $r^2 = 0.999$. Although the kinetic experiments were well reproducible, it is clear that the dependence of absorbance on time deviates from the ideal course of the first-order kinetic curve, which is also the cause of the significant standard deviations with which the respective rate constants were determined. The deformation of the kinetic curves was probably caused by subsequent reactions during the oxidation of AG25, the intermediate products of which significantly absorbed in the measured part of the UV-VIS spectrum. A separate direct determination of the rate constant of the AG25 chromophore decay is impractical given the similar reaction half-times of subsequent reactions.

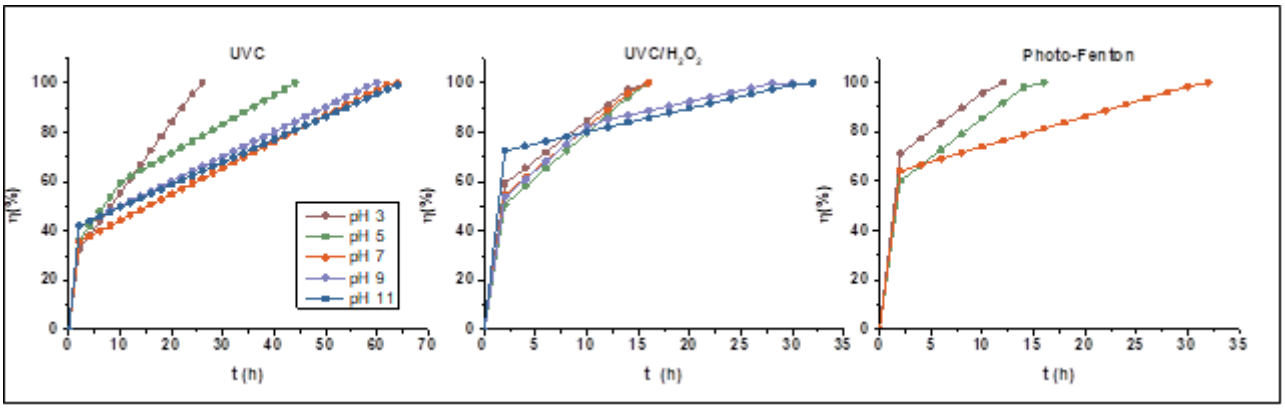

Figure 16 Dependence of the decrease in the original concentration (UV-C $3 \cdot 10^{-5}$ mol/L, UV-C/H_2O_2 and Photo-Fenton reaction $5 \cdot 10^{-5}$ mol/L) on time during decolorization of model wastewater containing Acid Green 25 for UV-C, UV-C/H2O2 reaction systems and photo-Fenton reaction. Spectrophotometric kinetic measurements were performed at t= 25 ◦C, λ_{anal}= 643 nm and in the pH range between 3-11

3.2.4. Acid Red 118

The decolorization kinetics of the AR118 dye was measured again as absorbance time dependences, from which the actual dye concentration as a function of time was calculated using the calibration curve equation $A_{492} = 0.1276c_{AR118}$, $r^2 = 0.998$. Even in this case, first-order kinetic equations are best suited to describe the reaction rates of AR118 decolorization. Decolorization of model water with AR118 using UV-C alone corresponds to k_{obs}=1.514·10-4±0.385·10^{-4} s^{-1} for pH 3 (corresponding to $t_{1/2}$= 1.5 h), for pH 5 this value increased to k_{obs}=2.367·10^{-4}±0.438·10^{-4} s^{-1} ($t_{1/2}$=0.8 h) and the slowest process took place at pH 9, where the k_{obs} value was 1.210·10^{-4}±0.122·10^{-4} s^{-1} with a corresponding reaction half-time $t_{1/2}$=1.6 h.

For the UV-C/H_2O_2 reaction system, the reaction appears to be fastest again at pH 5 (k_{obs}= 5.366·10^{-4} ±0.399·10^{-4} s^{-1} with $t_{1/2}$= 0.36 h). Unlike the previous system, this system appears to be the slowest at pH 7, where the k_{obs} value is 3.428·10^{-4} ±0.491·10^{-4} s^{-1} ($t_{1/2}$=0.57 h). The photo-Fenton reaction for the degradation of AR118 was not used due to the inhomogeneity of the solution. The reason is the interaction of iron ions with sulpho groups of AR118 to form insoluble ferrous and ferrous salts, and thus the impossibility of continuous measurement of the decrease in absorbance over time. Dependences of the decolorization efficiency of model wastewater containing Acid Red 118 and the dependence of the initial concentration decrease on time for the reaction systems UV-C, UV-C/H_2O_2 are shown in figure 17.

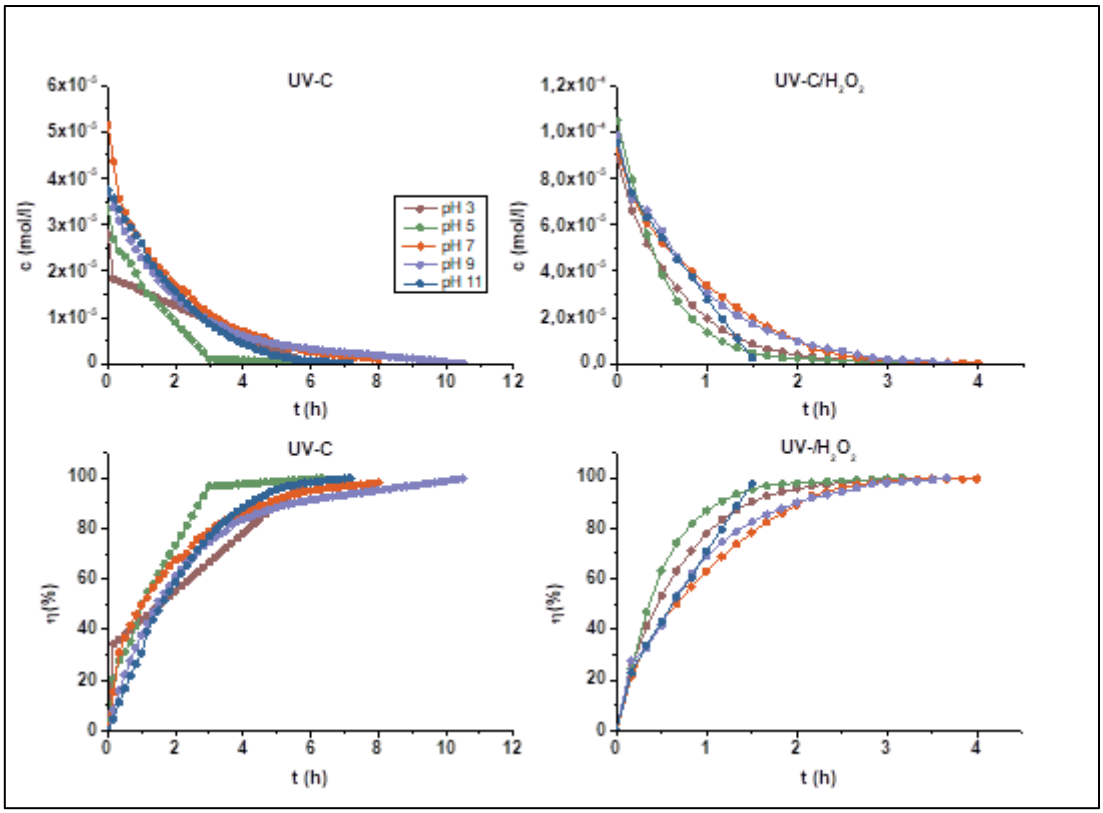

Figure 17 Dependences of the decolorization efficiency of model wastewater containing Acid Red 118 and the dependence of the initial concentration decrease on time for the reaction systems UV-C, UV-C/H_2O_2. Spectrophotometric kinetic measurements were performed at t= 25 ◦C, λ_{anal}= 492 nm and in the pH range between 3-11

Conclusion

When choosing a method for removing pollutants from wastewater, attention is paid especially to economic factors in combination with the efficiency of the processes used. The ecological problematic nature of textile and dyeing waters lies, as already mentioned, in the presence of stable organic dyes and a considerable number of inorganic salts. If an organic dye is a pollutant that we want to remove from wastewater together with dissolved salts, it is difficult to find a more suitable solution than membrane processes, due to their high separation efficiency at ambient temperature, lower energy consumption, space efficiency and economic acceptability as part of a long-term investment.

In this aspect, AOPs can also be used as an alternative to conventional water treatment based on the adsorption principle. However, their purpose is not to apply them for the primary treatment of exhausted dyeing baths and undiluted wastewater, e.g. from dye production, where at high concentrations of dyes (still in the order of units of g/l), the demands on reaction time and consequently the costs of generating the hydroxyl radical, regardless of the reaction system used, are still relatively high. Their application in the role of secondary purification process, following e.g. nanofiltration, is far more suitable. The choice of AOP process must be based on the reaction conditions, which can include the pH and temperature of the medium to be cleaned and the expected reaction rate of the process. For example, UV-C radiation itself is a non-thermal intervention of a technology using purely physical energy, which does not require high investment, maintenance and costs and is applicable in a wide pH range, but the reaction times are longer.

Based on these factors and the results of this work, we can easily say that both of these methods have proven to be very effective in removing textile dyes that are difficult to biodegrade. In the theoretical part, these methods and their principles were described in detail. The continuity of the experimental conditions of the tested membrane separation and AOP processes contributes to the modularity and usability of the obtained data in the field of environmental protection on an industrial scale.

List of References

[1] ALINSAFI, A., EVENOU, F., ABDULKARIM, E. M., PONS, M. N., ZAHRAA, O., BENHAMMOU, A., YAACOUBI, A., NEJMEDDINE, A. Treatment of textile industry wastewater by supported photocatalysis. *Dyes and Pigments*, Vol. 74 (2007), p. 439-445. ISSN 0143-7208.

[2] MIKULÁŠEK, P. a kol. (2013). *Tlakové membránové procesy*. Vysoká škola chemicko-technologická v Praze. ISBN 978-80-7080-862-7.

[3] SREBENKOSKA, V., ZHEZHOVA, S., RISTESKI S., SASKA, G. Methods for wastewaters treatment in textile industry. *International scientific conference UNITECH*, (2014), p. 248-252.

[4] MOSTAFA, M. Wastewater treatment in textile Industries - the concept and current removal technologies. *Journal of Biodiversity and Environmental Sciences*, Vol 7 (2015), p. 501-525. ISSN: 2220-6663.

[5] BABU, R. B., PARANDE, A. K., RAGHU, S., KUMAR, P.T. Textile Technology-Cotton Textile Processing: Waste Generation and Effluent Treatment. *The Journal of Cotton Science,* Vol. 11 (2007), p. 141-153.

[6] MULDER, M. (1996). *Basic Principles of Membrane Technology*. 2nd ed. Kluwer Academic Publishers: London.

[7] VERLIEFDE, A. R. D., CORNELISSEN, E.R., HEIJMAN, S. G. J., VERBERK, J., AMY, G. L., VAN DER BRUGGEN, B, VAN DIJK, J. C. J. *Membrane Science*, Vol. 322 (2008), p. 52-66. ISSN 0043-1354.

[8] VAN DER BRUGGEN, B., MANTTARI, M., NYSTROM, M. S*eparation and Purification Technoly*, Vol. 63 (2008). ISSN 1383-5866.

[9] HUSSAIN A.A, NATARAJ S.K., ABASHAR M.E.E., AL-MUTAZ I.S., AMINABHAVI T.M. Prediction of physical properties of nanofiltration membranes using experiment and theoretical models. *J. Membr. Sci.*, Vol. 310 (2008), p. 321–336. ISSN 0376-7388.

[10] PAVLÍK J. (2004). *Využití nanofiltrace v chemickém průmyslu*. Bakalářská práce. Univerzita Pardubice.

[11] Filmtec Membranes. *Basics of RO and NF: Membrane Description*. Tech Manual Excerpt.

[12] LITTER, M. I. (2005) *Introduction to Photochemical Advanced Oxidation Processes for Water Treatment*. Hdb Env Chem Vol. 2, p. 325–366, Springer-Verlag Berlin Heidelberg.

[13] CHAWLA, A., LOBACZ, A., TARAPATA, J., ZULEWSKA, J. UV Light Application as a Mean for Disinfection Applied in the Dairy Industry. *Appl. Sci.*, Vol. 11 (2021).

[14] JOSE, C., RODRIGUES. R., ANTONIO, C. S. C.(2018). *UV hydrogen peroxide processes*. Teixeira University of Salo Paulo, Chapter 2, p. 13- 49.

[15] AFONSO-OLIVARES, C., FERNANDEZ-RODRIGUEZ, C., OJEDA-GONZALES, R. J., SOS-FERRERA, Z., SANTANA-RODRIGUEZ, J. J., DONA RODRIGUEZ, J.M. Estimation of kinetic parameters and UV doses necessary to remove twenty-three pharmaceuticals from pre-treated urban wastewater by UV/H_2O_2. *J. Photochem. Photobiol. A,*Vol. 329 (2016) p. 130-138.

[16] HOU, H.; ZENG, X.; ZHANG, X.; Angew. Production of Hydrogen Peroxide by Photocatalytic Processes. *Chem. Int. Ed*, Vol. 59 (2020)

[17] GARCIA-FERNANDEZ, M., POLO-LOPEZ, I., OLLER, P. FERNANDEZ, I. Bacteria and fungi inactivation using Fe^{3+}/sunlight, H_2O_2/sunlight and near neutral photo-Fenton: A comparative study. *Applied Catalysis B. Environmental.,* Vol. 121 (2012), p. 20-29. ISSN 0926-3373.

[18] ÇALIK, C., ÇIFCI, D. I. Comparison of kinetics and costs of Fenton and photo-Fenton processes used for the treatment of a textile industry wastewater. *Journal of Environmental Management*, Vol. 304 (2022). ISSN 0301-4797.

[19] KRUPKOVÁ, O. *Pokročilé oxidační procesy s využitím peroxidu vodíku.* Diplomová práce. Univerzita Pardubice. Fakulta chemicko-technologická. 2020.

[20] PALARČÍK, J., KRUPKOVÁ, O., PEROUTKOVÁ, P., MALAŤÁK, J., VELEBIL, J., CHÝLKOVÁ, J., DUŠEK, L. Decolorization and Oxidation of Acid Blue 80 in Homogeneous and Heterogeneous Phases by Selected AOP Processes. Catalysis for the Removal of Water Pollutants. *Catalysts*, Vol. 12 (2022), no. 6, p. 644. ISSN 2073-4344.

[21] KUCHTOVÁ, G., CHÝLKOVÁ, J., VÁŇA, J., VOJS, M., DUŠEK, L. Electro-oxidative Decolorization and Treatment of Model Wastewater Containing Acid Blue 80 on Boron Doped Diamond and Platinum Anodes. *J. Electroanal. Chem*., Vol. 863 *(*2020). ISSN 1572-6657.

[22] KHATAEE, A. R., ZAREI, M., FATHINIA, M., KHOBNASAB JAFARI, M., Photocatalytic degradation of an anthraquinone dye on immobilized TiO_2 nanoparticlesin a rectangular reactor: Destruction pathway and response surface approach. *Desalination*, Vol. 268 (2011), p. 126-133. ISSN 0011-9164.

[23] OLUMIDE, B. A., TOGUNWA, O. S. Catalytic activity of copper modified bentonite supported ferrioxalateon the aqueous degradation and kinetics of mineralization of DirectBlue 71, Acid Green 25 and Reactive Blue 4 in photo-Fenton process. *Applied Catalysis*, Vol. 470 (2014), p. 285-293. ISSN 0011-9164.

[24] RADI, M. A., NASIRIZADEH, N., ROHANI-MOGHADAM, M., DEHGHANI, M. The comparison of sonochemistry, electrochemistry and sonoelectrochemistry techniques on decolorization of C.I Reactive Blue 49. *Ultrasonics Sonochemistry,* Vol. 27 (2015), p. 609-615. ISSN 1350-4177.

[25] ASGHER, M., BHATTI, H. N. Removal of Reactive Blue 19 and Reactive Blue 49 textile dyes by citrus waste biomass from aqueous solution: ekvilibrium and kinetic study. *The Canadian journal of chemical engineering*, Vol. 90 (2012), p. 412-419.

[26] RADI, M. A., NASIRIZADEH, N., MIRJALILI, M., ROHANI MOGHADAM, M. Ultrasound-assisted electrochemical decolorization of anthraquinone dye C.I Reactive Blue 49, its optimization and synergic efect: a comparative study. *International Journal of Environmental Science and Technology*, Vol. 16 (2019), p. 2455–2464.

[27] SEIDENARI, S., MANZINI, B. M., SCHOIAVI, M. E., MOTOLESE, A. Prevalence of contact allergy to non-disperse azo dyes for natural fibers: a study in 1814 consecutive patients. Contact Dermatitis, Vol. 33 (1995), p. 118-122.

[28] MAROUDAS, A., PANDIS, P. K., CHATZOPOULOU, A., DAVELLAS, L. R., SOURKOUNI, G., ARGIRUSIS, C. Synergetic decolorization of azo dyes using ultrasounds, photocatalysis and photo-fenton reaction, *Ultrasonics Sonochemistry*, Vol. 71 (2021). ISSN 1350-4177.

[29] KRUPKOVÁ, O., DUŠEK, L., CUHORKA, J., SOARES, G., KUCHTOVÁ, G., MIKULÁŠEK, P., BENDOVÁ, H. Removal of textile dye reactive blue 49 from wastewater and dye baths by membrane separation and subsequent photo-Fenton reaction, UV-C and UV-C/H_2O_2. *Journal of Water Process Engineering*. Vol. 65 (2024). ISSN 2214-7144.

List of Students' Published Works

Articles published in journals with IF

PALARČÍK, Jiří., KRUPKOVÁ, O., PEROUTKOVÁ, P., MALAŤÁK, J., VELEBIL, J., CHÝLKOVÁ, J., DUŠEK, L., Decolorization and Oxidation of Acid Blue 80 in Homogeneous and Heterogeneous Phases by Selected AOP Processes. Catalysis for the Removal of Water Pollutants. *Catalysts*, vol. 12, 2022, no. 6, s. 644. ISSN 2073-4344.

KRUPKOVÁ, O., DUŠEK, L., CUHORKA, J., SOARES, G., KUCHTOVÁ, G., MIKULÁŠEK, P., BENDOVÁ, H., Removal of textile dye reactive blue 49 from wastewater and dye baths by membrane separation and subsequent photo-Fenton reaction, UV-C and UV-C/H_2O_2, *Journal of Water Process Engineering*, vol. 65, 2024, s. 105735. ISSN 2214-7144.

Article published in university journal (student scientific professional activities)

KRUPKOVÁ, O., KOŘÍNKOVÁ, J., MACHALICKÝ, O., *Metody stanovení obsahu dithiokarbamátů u vybraných peckovin*. In Sborník příspěvků: studentská vědecká odborná činnost 2018/2019. Pardubice: Univerzita Pardubice, 2019. s. 107 – 111. ISBN 978-80-7560-260-2.

Participation in international conferences

KRUPKOVÁ, O., CUHORKA, J. ,DUŠEK, L. *Dye removal from aqueous solutions by nanofiltration*. In ChemZi. Bratislava: Slovenská chemická spoločnosť pri SAV, 2021. 34-37 s.

DUŠEK, L., CUHORKA, J., KRUPKOVÁ, O. *Removal of Acid Blue 80 from aqueous solutions by advanced oxidation processes and membrane processes*. In 3rd International Scientific Conference Ecological and Environmental Engineering: book of abstracts. Krakov: University of Agriculture, 2022. s. 79-80.

DUŠEK, L. - KUCHTOVÁ, G. - KRUPKOVÁ, O. *Degradation of Acid Green 25 in wastewater by advanced oxidation processes*. In 3rd International Scientific Conference Ecological and Environmental Engineering: book of abstracts. Krakov: University of Agriculture, 2022. s. 79-80.

Krupková, O., Dušek, L., *Degradation of textile dyes from wastewater by oxidation processes*. In ChemZi. Bratislava: Slovenská chemická společnosť pri SAV, 2023. S. 175. ISSN 1336-7242.

Participation in national conferences

KRUPKOVÁ, O., CUHORKA, J., DUŠEK, L. *Odstraňování barviv z vodných roztoků pomocí nanofiltrace*. Sanační technologie XXIII. Chrudim: Vodní zdroje Ekomonitor, spol. s r.o., 2021. 164-168 s. ISBN 978-80-88238-20-1.

KRUPKOVÁ, O.-DUŠEK, L. *Textilní barviva a jejich degradace z vodných roztoků*. Rosteme s chemií, Univerzita Pardubice, 2023. s. 36. ISBN: 978-80-7560-462-0.

KRUPKOVÁ, O., DUŠEK, L., CUHORKA, J., MIKULÁŠEK, P., BENDOVÁ, H., KUCHTOVÁ, G. Přetržení vazeb, které nemohou být navráceny aneb odstranění reaktivního barviva z odpadních vod. Rosteme s chemií. Praha. Univerzita Karlova, 2024. s. 39. ISBN: 978-80-7560-510-8.